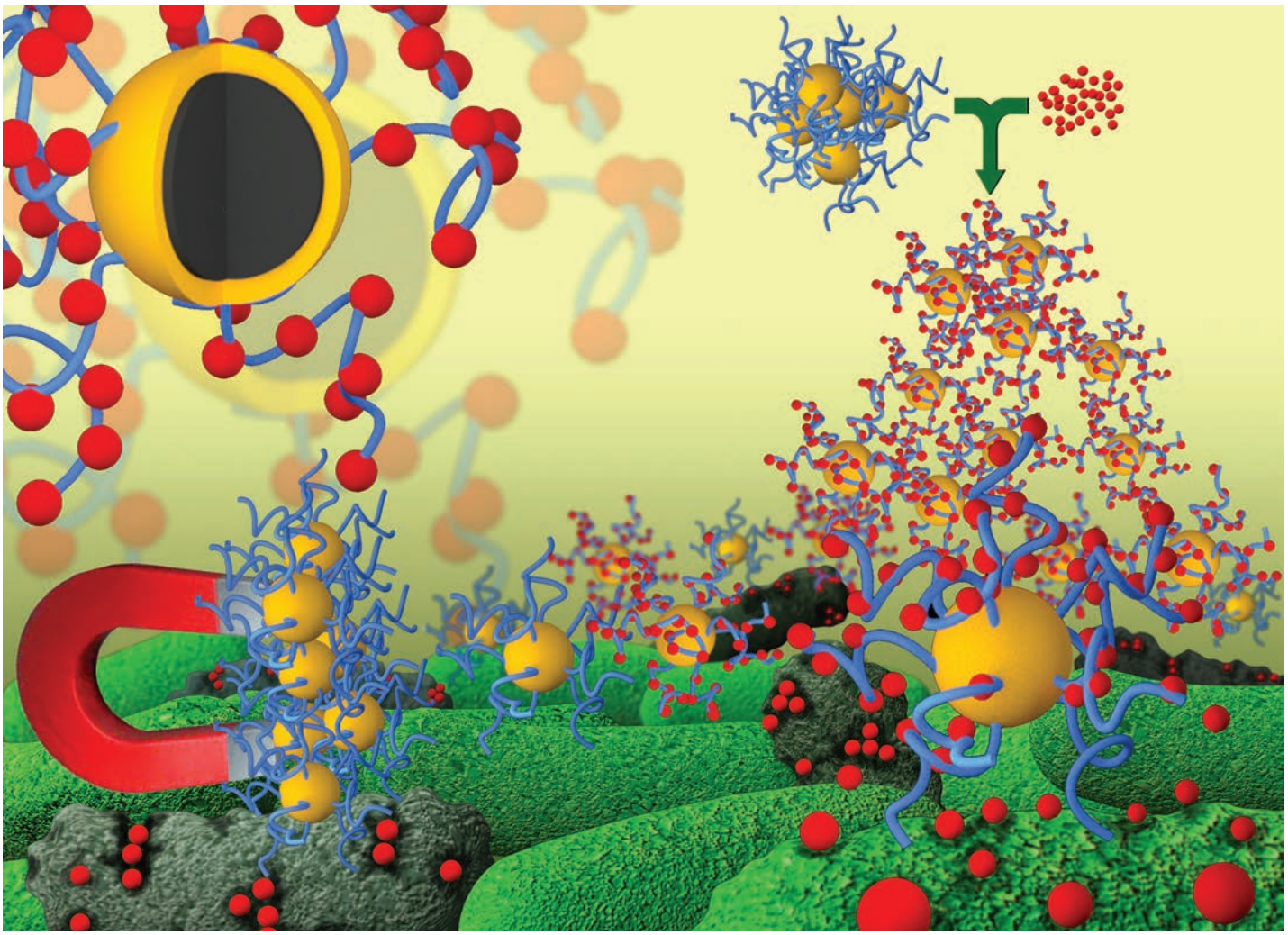

Highlighting research results from the University of South Carolina, Columbia, SC, United States.

Polymer grafted recyclable magnetic nanoparticles

Recyclable poly(methacrylic acid) grafted magnetic particles were prepared that retained excellent aqueous phase dispersibility when loaded with an antibiotic. The drug-nanoparticle complex showed enhanced biological activity against bacteria as compared to the free drug. The particles were removed from the environment using a magnet after killing bacteria, thus avoiding nano-based pollution of the biological environment.

As featured in:

See Brian C. Benicewicz *et al.* *Polym. Chem.*, 2015, **6**, 248.

ROYAL SOCIETY OF CHEMISTRY

www.rsc.org/polymers

Registered charity number: 207890

Polymer Chemistry

PAPER

View Article Online
View Journal | View Issue

Published on 22 September 2014. Downloaded by University of South Carolina Libraries on 01/04/2015 18:08:03.

Cite this: *Polym. Chem.*, 2015, **6**, 248

Polymer grafted recyclable magnetic nanoparticles†

Lei Wang,[a] Marcus Cole,[a] Junting Li,[a] Yang Zheng,[a] Yung Pin Chen,[b] Kristen P. Miller,[b] Alan W. Decho[b,c] and Brian C. Benicewicz*[a,c]

Received 17th August 2014,
Accepted 22nd September 2014

DOI: 10.1039/c4py01134a

www.rsc.org/polymers

This work reports on a new combination of recyclable magnetic nanoparticles, polymers and antibiotics that show increased effectiveness in combating bacterial infections. The direct-coprecipitation of iron salts strategy was used to generate superparamagnetic nanoparticles with a saturation magnetization of 59.5 emu g^{-1}. A silica coating was applied and used to stabilize the magnetic nanoparticles and create a convenient platform for further functionalization. A variety of PMAA brushes with different lengths and densities were prepared on the magnetic nanoparticles with an average diameter size as small as 10 nm *via* surface-initiated reversible addition fragmentation chain transfer (RAFT) polymerization of methacrylic acid. The polymer grafted magnetic nanoparticles were removed from water solutions after antimicrobial testing using a magnet, thereby avoiding nano-based pollution of the environment. The bioactivity of an antibiotic (penicillin-G) over bacteria (*Staphylococcus aureus* and *Escherichia coli*) was significantly enhanced when physically bound to the PMAA grafted magnetic nanoparticles. The inhibition activity of the penicillin-nanoparticle complex was retained using recycled magnetic nanoparticles that had been reloaded with penicillin-G.

Introduction

Nanomaterials have been widely used in various areas due to the unique properties.[1,2] Magnetic nanoparticles with controlled size and high magnetization are important materials with wide application in magnetic recording, magnetic resonance imaging (MRI), drug delivery and therapeutics.[3,4] However, there are some problems with the application of bare iron oxide nanoparticles in these fields, such as easy aggregation, rapid biologically-caused decomposition and the environmentally induced loss of the magnetic properties.[5] Silica coated iron oxide magnetic nanoparticles provide a biocompatible silica shell, which can effectively protect the iron oxide core in biological systems and preserve the magnetic properties. The silica coating is also a convenient platform for subsequent surface functionalization *via* a powerful silica surface chemistry toolbox.

Polymers are important materials with tunable properties,[6–9] which can be used to modify the surface of nanomaterials. A variety of polymers have been used to functionalize and stabilize iron oxide magnetic nanoparticles *via* various surface chemistries.[10,11] Controlled radical polymerization (CRP) has been used to prepare polymer materials with controllable molecular weights.[12–14] As an important CRP technique, reversible addition–fragmentation chain transfer (RAFT) polymerization has been widely applied to synthesize a variety of functional polymers with different architectures in a controlled manner (predictable molecular weights and low polydispersities).[15,16] RAFT polymerization has emerged as a powerful tool to modify nanoparticle surfaces to prepare polymer grafted nanoparticles with significant advantages, such as the applicability to many radical polymerizable monomers, low metal contamination in the final polymer, and mild polymerization conditions.[17–22] Polymer grafted nanoparticles have important applications in biomedical areas such as drug delivery and tumor therapy.[23]

Poly(methacrylic acid) (PMAA) represents an important class of pH-responsive polymers and has been used in membrane transport,[24] coatings,[25] sensors[26] and biomedical applications.[27] There are a few reports on the surface functionalization of nanoparticles with PMAA or other multi-acid containing polymers. Some research groups reported the strategy of deprotection of surface attached poly(*tert*-butylacrylate) or poly(*tert*-butylmethacrylate).[28–31] However, the depro-

[a]*Department of Chemistry and Biochemistry, University of South Carolina, Columbia, SC 29208, USA. E-mail: benice@sc.edu*
[b]*Department of Environmental Health Sciences, University of South Carolina, Columbia, SC 29208, USA*
[c]*USC NanoCenter, University of South Carolina, Columbia, SC 29208, USA*

†Electronic supplementary information (ESI) available: Fe_3O_4/SiO_2 magnetic nanoparticles and PMAA grafted magnetic nanoparticles. See DOI: 10.1039/c4py01134a

This journal is © The Royal Society of Chemistry 2015

Published on 22 September 2014. Downloaded by University of South Carolina Libraries on 01/04/2015 18:08:03.

tection of the *tert*-butyl moiety is tedious and usually uses harsh conditions. Thermal deprotection of poly(1-ethoxyethyl acrylate) and poly(2-(pyridin-2-yl)ethyl methacrylate) has been conducted to generate poly(acrylic acid) and PMAA respectively.[32,33] However, the thermal conditions may cause nanoparticle aggregation when the deprotection is conducted on particle surfaces. The direct surface-initiated polymerization of acid containing monomers on particles has been reported by very few groups.[34,35] However, these particles were very large (up to 11 μm diameter) and are not appropriate for many biomedical applications. Direct surface-initiated polymerization of acid containing monomers on small size nanoparticles that maintain good dispersibility is still a challenge for biomedical applications. RAFT polymerization is a versatile technique which can be used to mediate a variety of functional monomers while other CRP techniques (*e.g.* ATRP) cannot be used for acid containing monomers due to catalyst poison issues.[36] In this work, we report the investigation of the direct polymerization of MAA on small sized (10 nm) Fe_3O_4/SiO_2 magnetic nanoparticles *via* surface-initiated RAFT polymerization while maintaining good dispersibility in solutions and explore their use as recyclable drug delivery vehicles.

The alarming phenomenon of bacterial resistance to antibiotics causes high morbidity and mortality, which is an extremely critical problem in the healthcare area.[37] A variety of antibiotics used over several decades, such as penicillin, become much less active or inactive to bacterial strains. Nanoparticles have been used as drug delivery materials because of their unique properties, such as high specific surface area, nano-size effects and multiple surface engineering approaches to introduce new functionalities.[38]

Magnetic nanoparticles have exhibited a variety of advantages in biomedical applications.[3,4] The unique property of stimulus response under magnetic fields can be used to direct the antibiotic attached magnetic nanoparticles to penetrate complicated bacterial environments, such as biofilms, which are much more resistant to antibiotics than individual bacteria. Using the magnetic nanoparticles as a delivery platform also allows them to be easily recycled *via* a magnet without leaving residual nanomaterials in the environment which avoids public health concerns. Magnetic particles have been widely used as drug delivery vehicles to eukaryote cells; however, there are few reports on applications to bacterial cells. In addition, the recyclability of the delivery vehicles in bacterial systems has not yet been reported, even though antimicrobial poly(quaternary ammonium) grafted magnetic nanoparticles have been reported.[39] In this work, we used PMAA grafted magnetic nanoparticles as a recyclable platform, with a high surface area to volume ratio, to conjugate high localized concentrations of penicillin-G and examined their effectiveness in killing bacteria. The recyclability of the magnetic particles is also discussed.

The Fe_3O_4/SiO_2 magnetic nanoparticles were synthesized by two methods. The first strategy was a microemulsion method employing the mixing of two separate microemulsions (ME1 and ME2) resulting in the formation of nanoparticles

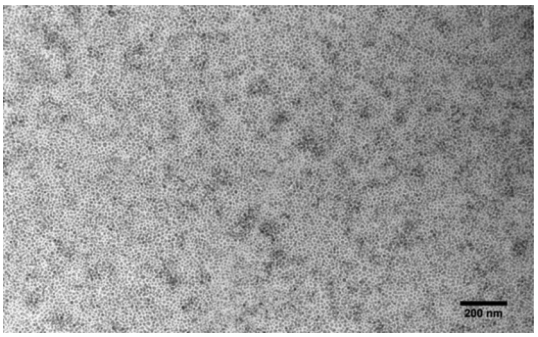

Fig. 1 TEM of Fe_3O_4/SiO_2 nanoparticles prepared by the microemulsion method.

(Table S1†). ME1 contained Triton X-100, cyclohexane, *n*-hexanol, water, TEOS, $FeCl_3$ and $FeSO_4$, while ME2 contained Triton X-100, cyclohexane, *n*-hexanol, water, TEOS and the base (NH_4OH).

The generated Fe_3O_4/SiO_2 nanoparticle solution was light brown and transparent. The TEM image (Fig. 1) illustrates that the Fe_3O_4/SiO_2 nanoparticles were well dispersed and shows that the diameter of the individual nanoparticles was approximately 11 nm. The colors of the nanoparticles (Fig. 2) varied from dark brown to light yellow. The lighter color of the magnetic nanoparticles was observed in compositions containing higher amounts of TEOS. The nanoparticles with 10× TEOS have higher weight loss (18.6%) compared to the particles with 5× TEOS (17.3% weight loss) at 940 °C in TGA analysis. Increasing the proportion of TEOS would be helpful to enhance the SiO_2 part of the nanoparticles. Even though well-dispersed nanoparticles were obtained using the microemulsion method, the nanoparticles did not have high saturation magnetization (less than 5 emu g^{-1}) and strong magnetic responses, similar to other Fe_3O_4/SiO_2 magnetic nanoparticles.[5] Thus, we were motivated to develop a new strategy to prepare Fe_3O_4/SiO_2 magnetic nanoparticles with high magnetization, excellent dispersity, and small size.

The second strategy was based on the coprecipitation of Fe^{2+} and Fe^{3+} salts in basic aqueous solutions at low temperatures to form nanoparticles. Fe(III) and Fe(II) salts were co-precipitated with NH_4OH at 90 °C to form iron oxide nanoparticles followed by the hydrolysis of TEOS on the Fe_3O_4 nanoparticle surface to form Fe_3O_4/SiO_2 magnetic nanoparticles. The XRD pattern (Fig. 3) confirmed the non-crystalline SiO_2 shell ascribed to the broad peak at 10°–30° and the cubic

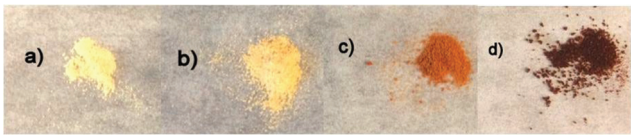

Fig. 2 Photograph of Fe_3O_4/SiO_2 nanoparticles prepared *via* the microemulsion method: (a) 10× TEOS of the standard recipe; (b) 5× TEOS of the standard recipe; (c) standard recipe; (d) 2× iron of the standard recipe.

Published on 22 September 2014. Downloaded by University of South Carolina Libraries on 01/04/2015 18:08:03.

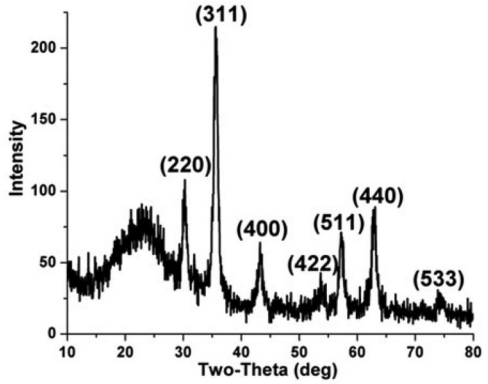

Fig. 3 XRD of Fe_3O_4/SiO_2 magnetic nanoparticles.

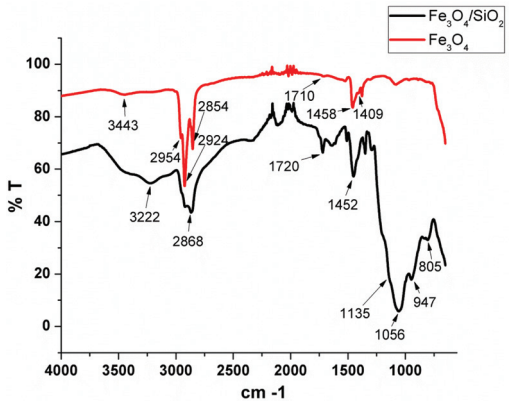

Fig. 4 IR of Fe_3O_4/SiO_2 and Fe_3O_4 magnetic nanoparticles.

spinel structure of Fe_3O_4 due to the strong diffraction peaks at 30.1°, 35.6°, 43.2°, 53.9°, 57.2°, 62.8°, and 74.2° which were indexed to (220), (311), (400), (422), (511), (440) and (533) planes, respectively. The IR analysis of Fe_3O_4 (Fig. 4) confirmed the absorption peaks at 2924 cm^{-1}, 2854 cm^{-1}, and 1710 cm^{-1} ascribed to the $-CH_2$ and C═O of the oleic acid physically absorbed on the Fe_3O_4 surface respectively. The peak at 1409 cm^{-1} revealed chemically bound oleic acid on Fe_3O_4 ascribed to the stretch of COO^- resulting from the coordination with iron of Fe_3O_4.[40] The IR spectra of Fe_3O_4/SiO_2 demonstrated the existence of SiO_2 after surface hydrolysis of TEOS on Fe_3O_4 nanoparticles based on the appearance of strong absorption peaks at 1135 cm^{-1}, 1056 cm^{-1}, 947 cm^{-1} and 805 cm^{-1}. The magnetic nanoparticle solution was dark brown and the nanoparticle powder (after washing and drying) was capable of lifting a medium size (1.5 cm diameter, 0.9 cm thickness) magnet off the ground, which qualitatively demonstrated the high magnetic moment of the as-synthesized magnetic nanoparticles (Fig. 5). A vibrating sample magnetometer (VSM) was employed to determine the magnetization strength of the magnetic nanoparticles (Fig. 6). The VSM measurement demonstrated the superparamagnetivity of both Fe_3O_4 and Fe_3O_4/SiO_2 nanoparticles with a high magnetic moment of 59.5 emu g^{-1} and 29.1 emu g^{-1} respectively. The silica coated

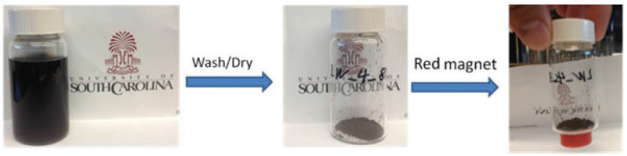

Fig. 5 General procedure for fabrication of Fe_3O_4/SiO_2 magnetic nanoparticles.

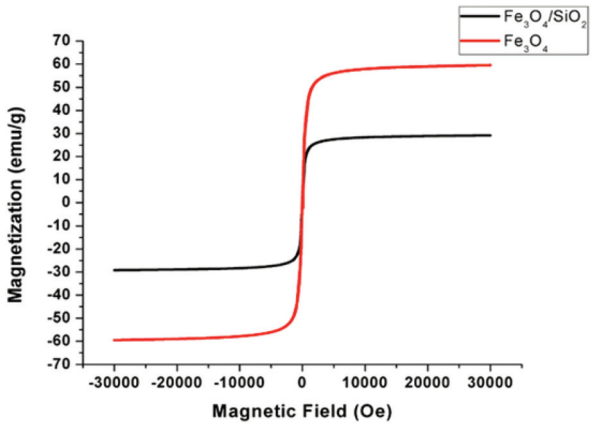

Fig. 6 VSM of superparamagnetic Fe_3O_4 nanoparticles (59.5 emu g^{-1}) and Fe_3O_4/SiO_2 nanoparticles (29.1 emu g^{-1}).

nanoparticles possess a lower magnetic moment than the bare Fe_3O_4, which is consistent with reports from other groups.[3] The TGA showed that the weight loss of Fe_3O_4/SiO_2 nanoparticles (after the addition of SiO_2 on Fe_3O_4) was 35% at 900 °C, which is significantly higher than the 24% of bare Fe_3O_4 nanoparticles (Fig. 7). The TEM image (Fig. 8) illustrates that the Fe_3O_4/SiO_2 nanoparticles were well-dispersed. The average diameter of the Fe_3O_4/SiO_2 nanoparticles was around 10 nm. Compared to the traditional strategy using thermal decomposition of a Fe(III) chelate in a high boiling point solvent (>200 °C),[4] this method uses much more mild synthetic con-

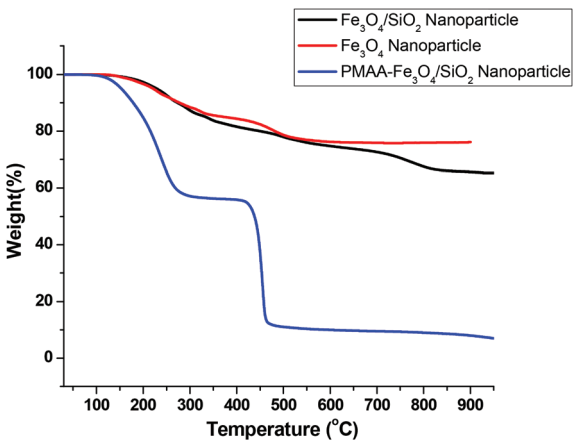

Fig. 7 TGA of Fe_3O_4, Fe_3O_4/SiO_2, and PMAA grafted Fe_3O_4/SiO_2 magnetic nanoparticles.

This journal is © The Royal Society of Chemistry 2015

Published on 22 September 2014. Downloaded by University of South Carolina Libraries on 01/04/2015 18:08:03.

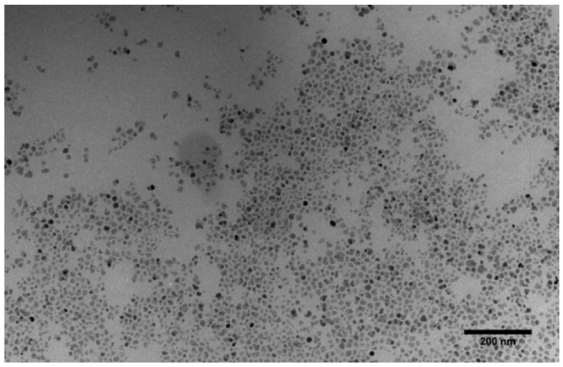

Fig. 8 TEM of Fe_3O_4/SiO_2 nanoparticles.

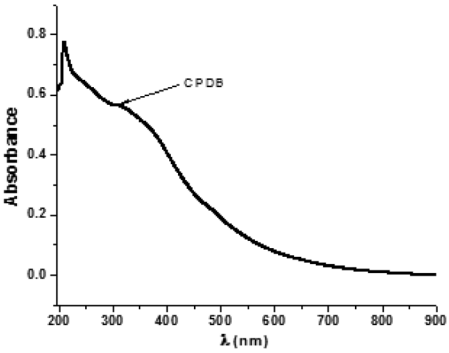

Fig. 9 CPDB coated Fe_3O_4/SiO_2 nanoparticles.

ditions and still provides high-magnetization superparamagnetic nanoparticles of small size.

The strategy for preparation of PMAA grafted Fe_3O_4/SiO_2 magnetic nanoparticles is shown in Scheme 1. Amino coated Fe_3O_4/SiO_2 nanoparticles were prepared by the reaction between as-synthesized Fe_3O_4/SiO_2 particles and 3-aminopropyldimethylethoxysilane. The RAFT agent coated Fe_3O_4/SiO_2 nanoparticles were synthesized by allowing the amino coated Fe_3O_4/SiO_2 nanoparticles with accurately determined densities to react with an excess of activated CPDB. This method generated a universal platform for surface initiated RAFT polymerization of nanoparticles with magnetic properties. The CPDB covalently bound to the nanoparticle surface was confirmed *via* UV-vis absorption at 305 nm (Fig. 9). A variety of CPDB coated Fe_3O_4/SiO_2 magnetic nanoparticles with different grafting densities (350 μmol g^{-1}, 151 μmol g^{-1}, 138 μmol g^{-1}), as determined by TGA, were prepared. Finally, the surface-initiated RAFT polymerization of MAA was conducted in DMF to generate PMAA brushes grafted onto magnetic nanoparticles.

Surface-initiated RAFT polymerization of MAA directly on Fe_3O_4/SiO_2 nanoparticles was conducted in DMF at 65 °C with a ratio between species of [MAA] : [CPDB] : [AIBN] = 1000 : 1 : 0.1. The PMAA grafted Fe_3O_4/SiO_2 nanoparticles were methylated by trimethylsilyldiazomethane followed by cleavage of the methylated chains from the nanoparticle surface with hydrofluoric acid solution to conduct accurate measurement of the molecular weights *via* organic phase (THF) GPC characterization. The molecular weight (M_n) of the attached PMAA chains was 58 302 g mol^{-1} and the PDI was 1.13. Another set of nanoparticles was prepared with surface attached short PMAA chains with a M_n = 12 900 g mol^{-1} and PDI was 1.04. The FTIR analysis of the methylated polymer grafted nanoparticles (Fig. 10) confirmed the appearance of the strong absorption peak at ~2951 cm^{-1} due to the generated methyl moiety. Additionally, the absence of a broad peak at 3500–2500 cm^{-1} due to the hydroxyl group in –COOH and the shift of the carbonyl stretch peak from 1700 cm^{-1} to 1729 cm^{-1} confirmed the successful methylation of the polymer chains. The TGA demonstrated that the surface anchored PMAA accounted for 91% by weight (Fig. 7). The PMAA grafted Fe_3O_4/SiO_2 nanoparticle solution was brown and transparent in dimethylformamide (DMF) (Fig. 11). The magnetic nanoparticles had a strong magnetic responsive property and could be easily redispersed in DMF after sonication maintaining the excellent dispersity in solution for at least 2 weeks. The grafted magnetic nanoparticles also readily dispersed in water. The AFM image (Fig. 12) reveals that the PMAA grafted

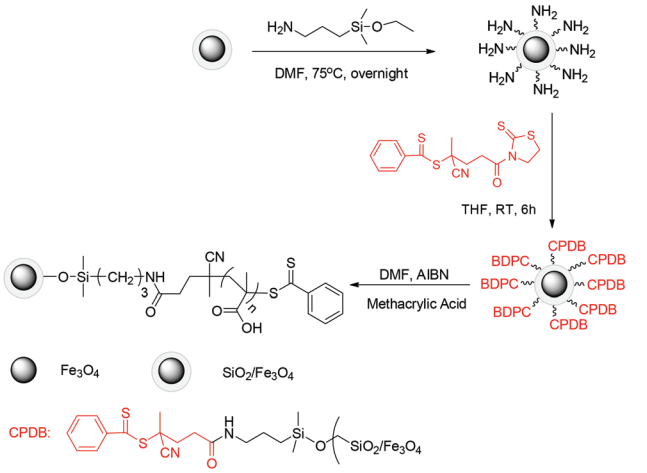

Scheme 1 Synthetic scheme for preparation of PMAA grafted Fe_3O_4/SiO_2 nanoparticles *via* direct polymerization of MAA.

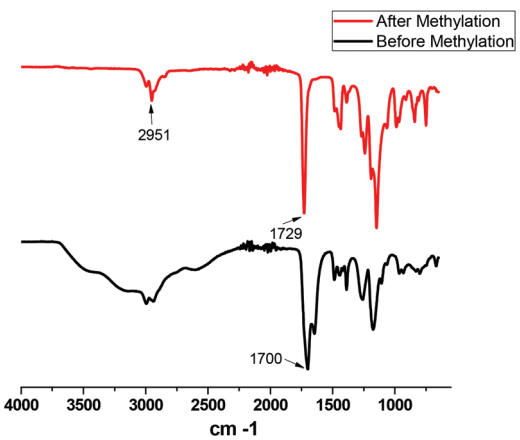

Fig. 10 IR spectra of PMAA grafted Fe_3O_4/SiO_2 magnetic nanoparticles before and after methylation.

Published on 22 September 2014. Downloaded by University of South Carolina Libraries on 01/04/2015 18:08:03.

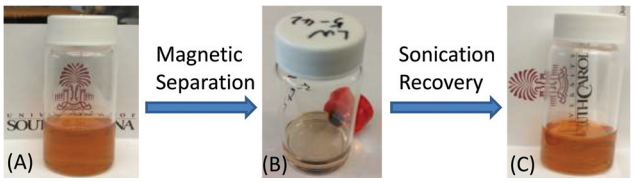

Fig. 11 PMAA grafted SiO_2/Fe_3O_4 nanoparticles in DMF: (A) normal state; (B) after magnetic separation; (C) sonication recovery and 14 days later.

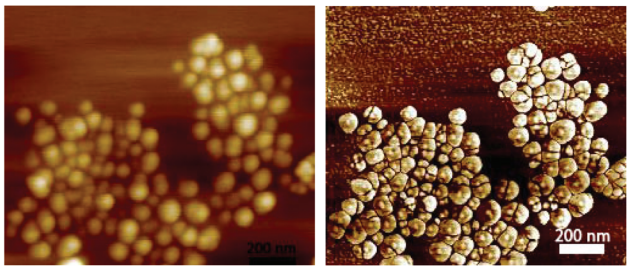

Fig. 12 AFM of PMAA grafted Fe_3O_4/SiO_2 magnetic nanoparticles. Left: phase image; right: height image. Size bar = 200 nm.

Fe_3O_4/SiO_2 hybrid nanoparticles were well dispersed, and shows that the size of the individual nanoparticles was around 40–50 nm, which is consistent with the TEM image (Fig. S1†).

The PMAA grafted magnetic nanoparticles were used to physically bind the beta-lactam antibiotic penicillin-G (PenG) and subsequently tested against bacteria. *Escherichia coli* (Gram-negative) and *Staphylococcus aureus* (Gram-positive) were selected as the target pathogens. The disk diffusion assay of the PenG-nanoparticle complex was conducted with a control group of the same dose of free PenG. In addition, as another control group, unloaded PMAA grafted magnetic nanoparticles demonstrated no activity (toxicity) towards both *E. coli* and *S. aureus*. The results (PenG dose was 12 μg) showed that the inhibition zone diameter of free PenG was 18 mm while the inhibition zone diameter of the PenG-nanoparticle complex was 23 mm (27.8% increase), which demonstrated that nanoparticle conjugated PenG possessed enhanced antimicrobial activity against *Staphylococcus aureus*. For the Gram-negative bacterium *Escherichia coli*, similar trends were also observed using a variety of PenG doses (Fig. 13). Thus, PMAA grafted magnetic nanoparticles enhanced the bioactivity of PenG against bacteria when the nanoparticles were physically bound with PenG. We hypothesize that the increased antimicrobial activity is ascribed to locally high concentrations of antibiotics bound to nanoparticles, which overwhelms the resistance of bacterial strains. The magnetic properties also offer a valuable stimulus technique to direct the nanoparticles in complicated bacterial environments, such as biofilms, while free antibiotics are not able to access cells in the sticky extracellular polymeric substances (EPS) of biofilms.

The culture solution method was used to evaluate the recyclability of PMAA grafted magnetic nanoparticles for antibiotic delivery and their effectiveness in killing bacteria. As a

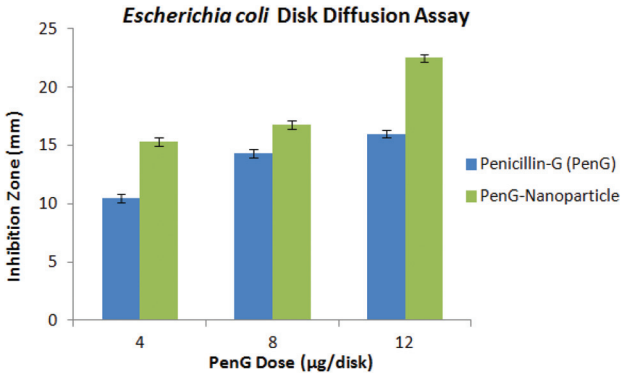

Fig. 13 Inhibition activity of free-PenG (blue), and PenG complexed to carboxylated polymers on magnetic nanoparticles (green) as tested by the disk diffusion method with *E. coli*. The PenG-nanoparticle complex had an equal amount of PenG as the free-PenG group at different PenG concentrations.

control group, the unloaded PMAA grafted nanoparticles exhibited no activity towards *E. coli* under the experimental conditions. The PenG-nanoparticle complex was added to the tryptic soy broth based *E. coli* culture solution with shaking at 37 °C. After overnight incubation, the bacterial growth of the suspension was determined by recording the absorbance at OD_{600}, and was compared with the standard bacterial culture solution without PenG and nanoparticles. Another control group of free PenG was tested in the same manner.

The PMAA grafted magnetic nanoparticles can be readily extracted and recycled using a magnet. The nanoparticles were attracted at the bottom of the tube *via* a magnet and the supernatant was removed. The collected nanoparticles were washed several times and used again to bind PenG and tested again for their ability to kill bacteria employing the above mentioned method (Scheme 2). The enhanced inhibition efficiency of the

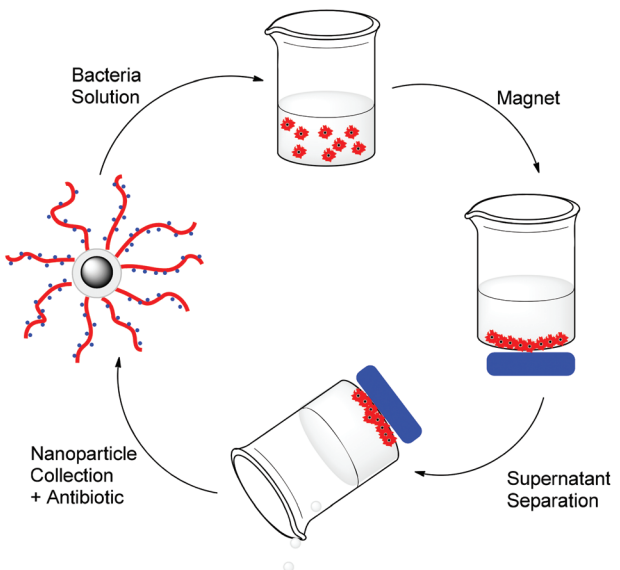

Scheme 2 Scheme of recycling magnetic nanoparticles to conjugate antibiotics for killing bacteria.

This journal is © The Royal Society of Chemistry 2015

Published on 22 September 2014. Downloaded by University of South Carolina Libraries on 01/04/2015 18:08:03.

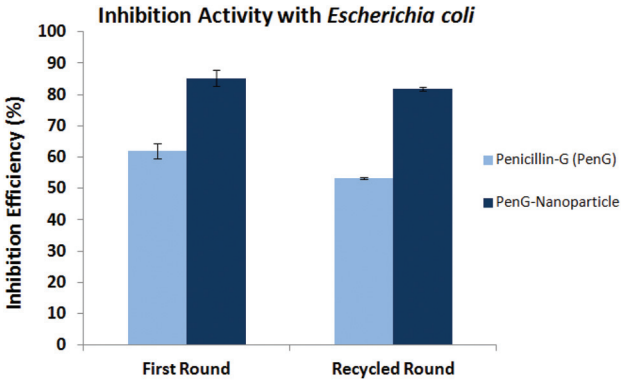

Fig. 14 Inhibition activities of free-PenG (light blue), and PenG complexed to carboxylated polymers on magnetic nanoparticles (navy) as tested by bacterial culture solution with *E. coli*.

PenG-nanoparticle complex using the recycled magnetic nanoparticles was retained, which again was much higher than the free PenG (Fig. 14). Similar to the previous testing protocol, the two groups had the same amount of PenG. We postulate that the effect is due to the locally high concentration of PenG bound to nanoparticles, which increases the effectiveness of the PenG to overcome bacterial resistance.

Experimental

Materials

Unless stated otherwise, all chemicals were purchased from Fisher Scientific or Sigma Aldrich and used as-received. Trimethylsilyldiazomethane (2.0 M in hexanes) was purchased from TCI. Activated 4-cyanopentanoic acid dithiobenzoate (CPDB) was prepared based on the literature.[41] Methacrylic acid (99.5%, Acros) was passed through an activated neutral alumina column to remove inhibitors. The initiator AIBN was purified *via* recrystallization in methanol before use.

Instrumentation

The Varian Mercury spectrometer 300/400 was used to record the ^{1}H NMR spectra using CD_3OD as the carrier solvent. Molecular weights and polydispersity index (PDI) were measured using a Polymer Labs PL-GPC-120 gel permeation chromatograph (GPC) associated with a 515 HPLC pump, a 2410 refractive index detector, and three Styragel columns. The columns consisted of HR1, HR3 and HR4 which have the corresponding effective molecular weight ranges of 100–5000, 500–30 000, and 5000–500 000, respectively. The GPC used tetrahydrofuran (THF) as the eluent at 30 °C and a flow rate of 1.0 mL min^{-1} with the calibration of poly(methyl methacrylate) or polystyrene standards obtained from Polymer Laboratories. Trimethylsilyldiazomethane was used to methylate the PMAA grafted nanoparticles[42] and the resulting polymer brushes were then cleaved with hydrofluoric acid (HF) for GPC characterization. Microfilters with a pore size of 0.2 μm were used to filter samples before GPC injection. Infrared spectra were measured with a BioRad Excalibur FTS3000 spectrometer. A Perkin-Elmer Lambda 4C UV-vis spectrophotometer was used to determine the UV-vis spectra. XRD characterization was conducted using a Rigaku D/Max 2100 powder X-ray diffractometer with Cu Kα radiation. TEM characterization was conducted using a Hitachi H8000 scanning transmission electron microscope with an accelerating voltage of 200 kV. The saturation magnetization of nanoparticles was determined using a Vibrating Sample Magnetometer (VSM). Tapping mode AFM characterization was conducted using a Multimode Nanoscope III system (Digital Instruments, Santa Barbara, CA). The system has commercial Si cantilevers with a spring constant and resonance frequency of 20–80 N m^{-1} and 230–410 kHz respectively. The sample of magnetic nanoparticles was prepared on silicon wafers *via* spin-coating. TGA characterization was operated using a TA Instruments Q5000 with a heating rate of 10 °C min^{-1} from 25 °C to 950 °C under nitrogen flow. Dynamic Light Scattering (DLS) characterization was operated using a Malvern Zetasizer Nano ZS90 instrument.

Synthesis of Fe_3O_4/SiO_2 magnetic nanoparticles

Two methods were employed to prepare Fe_3O_4/SiO_2 magnetic nanoparticles. The first method was a microemulsion strategy reported previously.[5] The second method was based on the following procedure: 6.94 g $FeCl_3$ and 6.04 g $FeSO_4{\cdot}7H_2O$ were dissolved in 400 mL N_2 purged DI water. To this solution was added slowly 15 mL 29 wt% NH_4OH at 90 °C under N_2 protection. Then, 9 mL oleic acid was added dropwise 1 hour later and the resulting solution was stirred at 90 °C for 2 hours. The solution was precipitated into a large amount of acetone to remove extra oleic acid. Then, Triton X-100 (2.5 mL) and 42 mL cyclohexane were added to a 250 mL round-bottom flask. After sonication for 1 min, 1 mL of the above prepared cyclohexane solution of Fe_3O_4 with a concentration of 22.4 mg mL^{-1} and 350 μL 29 wt% NH_4OH were added slowly to the stirring solution at room temperature (RT). TEOS was added slowly and the resulting solution was stirred at RT for 18 hours. The final solution was washed with methanol to remove the surfactant by precipitation and centrifugation at 4000 rpm for 5 min, which was repeated 4 times.

Synthesis of amino-functionalized Fe_3O_4/SiO_2 magnetic nanoparticles

3-Aminopropyldimethylethoxysilane (1.29 g, 8.0 mmol) was added to Fe_3O_4/SiO_2 nanoparticles (approx. 112 mg) dispersed in dry DMF (15 mL). The reaction mixture was stirred at 75 °C overnight under N_2 protection. The solution was precipitated into diethyl ether (200 mL), centrifuged at 3000 rpm for 5 minutes, and redispersed in dry THF. The solution was precipitated again into hexane and redispersed in dry THF for further use.

Synthesis of CPDB-functionalized Fe_3O_4/SiO_2 magnetic nanoparticles

Activated CPDB (202.4 mg, 532 mmol) was dissolved in dry THF (10 mL). The above amino-functionalized nanoparticles

Published on 22 September 2014. Downloaded by University of South Carolina Libraries on 01/04/2015 18:08:03.

(approx. 110 mg, in 20 mL THF) were added slowly and the resulting solution was stirred at RT overnight. After the reaction, the solution was precipitated into a cyclohexane and ethyl ether mixture (200 mL, cyclohexane–ethyl ether = 4 : 1), centrifuged at 3000 rpm for 5 minutes, and redispersed in dry DMF. The solution was precipitated again into ethyl ether and redispersed in dry DMF. This procedure was repeated several times until the supernatant solution was colorless after centrifugation. The final nanoparticles were dispersed in dry DMF for further usage.

Surface-initiated RAFT polymerization of methacrylic acid from CPDB anchored Fe_3O_4/SiO_2 nanoparticles

Methacrylic acid (0.99 mL, 1.17×10^{-2} mol), CPDB coated Fe_3O_4/SiO_2 nanoparticles (17 mg) and dry DMF (2.88 mL) were added to a 20 mL Schlenk tube. After sonication for 1 min, AIBN (233 μL, 5 mM in DMF) was added. The solution was degassed by four freeze–pump–thaw cycles, filled with nitrogen, and then placed in an oil bath of 65 °C for various intervals. The polymerization was stopped by quenching in ice water.

Synthesis of the PenG-nanoparticle complex

33 μl of PMAA grafted nanoparticles (35 mg ml^{-1}) was added to 500 μl of penicillin solution (1 mg ml^{-1}), followed by an incubation at 25 °C with shaking (280 rpm) for 2 hours. The resulting PenG-nanoparticle complex was collected *via* Amicon centrifuge tubes after the centrifugation at 10 000 rpm for 6 min. The complex was resuspended and washed *via* the centrifugation. The un-bound PenG amounts in the supernatant were negligible in the UV-vis analysis. Therefore, it was assumed that the majority of the PenG was conjugated to PMAA grafted nanoparticles.

Disk diffusion assay

Escherichia coli ATCC 25922 and *Staphylococcus aureus* ATCC 25423 were allowed to grow in 10 mL of tryptic soy broth (TSB) at 37 °C overnight to an optical density of 0.8 (OD_{600} = 0.8) and then diluted 10-fold. 0.1 mL of the diluted culture was used to inoculate an agar plate. 6 mm disks were put on the plate surface, and then a free PenG or PenG-nanoparticle complex DMSO solution (30 μL) was added to the disks at different concentrations. The plates were allowed to incubate at 35 °C and the clear zone surrounding a disk represents the areas that bacteria were killed. Each test was conducted in duplicate.

Bacteria inhibition efficiency determination

10 μl of *E. coli* suspensions (stock solutions, OD_{600} = 0.8) were inoculated into 2 mL TSB solutions at 37 °C for incubation at 300 rpm overnight. Three tubes of the same bacterial culture solutions were prepared. Tube 1 was used as the blank group without adding any PenG or nanoparticles. Tube 2 was employed to test the activity of free PenG. 50 μl of the PenG-nanoparticle complex (3.52 mg) was added to Tube 3 before incubation. Bacterial growth was measured at OD_{600}, and was compared with the Tube 1. Thus, the inhibition efficiency was calculated as follows: inhibition efficiency (%) = (Sample OD_{600}/Background OD_{600}) × 100. The Background OD_{600} was determined from Tube 1. Each test was conducted in duplicate.

Conclusions

In conclusion, we demonstrated an effective method for the preparation of Fe_3O_4/SiO_2 superparamagnetic nanoparticles with sizes as low as 10 nm and a high saturation magnetization using very mild synthetic conditions. CPDB coated Fe_3O_4/SiO_2 magnetic nanoparticles were prepared by treating amino functionalized Fe_3O_4/SiO_2 nanoparticles with activated CPDB. The direct surface-initiated RAFT polymerization of MAA was conducted on very small size Fe_3O_4/SiO_2 superparamagnetic nanoparticles while maintaining good dispersibility in solutions. The synthesis of the magnetic nanoparticles was confirmed by FTIR, TGA, VSM, TEM and AFM. The PMAA grafted Fe_3O_4/SiO_2 magnetic nanoparticles enhanced the bioactivity of PenG over bacteria (*Staphylococcus aureus* and *Escherichia coli*) when physically bound with PenG. The particles were removed from water solutions using a magnet after antimicrobial testing, thus avoiding nano-based pollution of the biological environment. The recycled PMAA grafted magnetic particles retained excellent aqueous phase dispersibility and high biological activity against bacteria when loaded with fresh PenG. The small size PMAA grafted magnetic nanoparticles with precisely controllable surface polymer brush lengths and PDIs provide an important platform to restore the activities of ineffective antibiotics *via* a new combination of materials to overcome bacterial resistance. The water-soluble PMAA grafted Fe_3O_4/SiO_2 magnetic nanoparticles may also find broad applications in MRI, and multiple drug delivery and therapeutic fields.

Acknowledgements

The authors would like to gratefully acknowledge Longfei Ye and Dr Thomas M. Crawford at the University of South Carolina (USC) for the VSM characterization, Rui Tan at USC for the TEM image editing, and the NSF (BME-1032579) for support of this work.

Notes and references

1 J. H. Liu and X. W. Liu, *Adv. Mater.*, 2012, **24**, 4097–4111.
2 J. H. Liu, J. S. Chen, X. F. Wei, X. W. Lou and X. W. Liu, *Adv. Mater.*, 2011, **23**, 998–1002.
3 T. Fried, G. Shemer and G. Markovich, *Adv. Mater.*, 2001, **13**, 1158–1161.
4 N. Pothayee, N. Pothayee, N. Jain, N. Hu, S. Balasubramaniam, L. Johnson, R. Davis, N. Sriranganathan and J. Riffle, *Chem. Mater.*, 2012, **24**, 2056–2063.

 This journal is © The Royal Society of Chemistry 2015

Published on 22 September 2014. Downloaded by University of South Carolina Libraries on 01/04/2015 18:08:03.

5 S. Santra, R. Tapec, N. Theodoropoulou, J. Dobson, A. Hebard and W. Tan, *Langmuir*, 2001, **17**, 2900–2906.
6 L. Ren, C. G. Hardy, S. Tang, D. B. Doxie, N. Hamidi and C. Tang, *Macromolecules*, 2010, **43**, 9304–9310.
7 J. Wang, J. Yu, Y. Liu, Y. Chen, C. Wang, C. Tang and F. Chu, *Green Mater.*, 2013, **1**, 105–113.
8 Y. Xu, W. W. Xu, M. D. Smith and L. S. Shimizu, *RSC Adv.*, 2014, **4**, 1675–1682.
9 J. Wang, Y. P. Chen, K. Yao, P. A. Wilbon, W. Zhang, L. Ren, J. Zhou, M. Nagarkatti, C. Wang, F. Chu, X. He, A. W. Decho and C. Tang, *Chem. Commun.*, 2012, **48**, 916–918.
10 C. Boyer, V. Bulmus, P. Priyanto, W. Y. Teoh, R. Amal and T. P. Davis, *J. Mater. Chem.*, 2009, **19**, 111–123.
11 C. Boyer, M. R. Whittaker, V. Bulmus, J. Liu and T. P. Davis, *NPG Asia Mater.*, 2010, **2**, 23–30.
12 L. Ren, C. G. Hardy and C. Tang, *J. Am. Chem. Soc.*, 2010, **132**, 8874–8875.
13 J. Wang, K. Yao, A. L. Korich, S. Li, S. Ma, H. J. Ploehn, P. M. Iovine, C. Wang, F. Chu and C. Tang, *J. Polym. Sci., Part A: Polym. Chem.*, 2011, **49**, 3728–3738.
14 Y. Xu, C. M. Thurber, T. P. Lodge and M. A. Hillmyer, *Macromolecules*, 2012, **45**, 9604–9610.
15 J. Chiefari, Y. K. Chong, F. Ercole, J. Krstina, J. Jeffery, T. P. T. Le, R. T. A. Mayadunne, G. F. Meijs, C. L. Moad, G. Moad, E. Rizzardo and S. H. Thang, *Macromolecules*, 1998, **31**, 5559–5562.
16 Y. Xu, C. M. Thurber, C. W. Macosko, T. P. Lodge and M. A. Hillmyer, *Ind. Eng. Chem. Res.*, 2014, **53**, 4718–4725.
17 L. Wang and B. C. Benicewicz, *ACS Macro Lett.*, 2013, **2**, 173–176.
18 J. Moraes, K. Ohno, T. Maschmeyer and S. Perrier, *Chem. Mater.*, 2013, **25**, 3522–3527.
19 Y. Li, T. M. Krentz, L. Wang, B. C. Benicewicz and L. S. Schadler, *ACS Appl. Mater. Interfaces*, 2014, **6**, 6005–6021.
20 R. Ranjan and W. J. Brittain, *Macromol. Rapid Commun.*, 2007, **28**, 2084–2089.
21 L. Wang, Y. P. Chen, K. Miller, B. M. Cash, S. Jones, S. Glenn, B. C. Benicewicz and A. W. Decho, *Chem. Commun.*, 2014, **50**, 12030–12033.
22 C. Boyer, M. H. Stenzel and T. P. Davis, *J. Polym. Sci., Part A: Polym. Chem.*, 2011, **49**, 551–595.
23 R. Mout, D. F. Moyano, S. Rana and V. M. Rotello, *Chem. Soc. Rev.*, 2012, **41**, 2539–2544.
24 A. M. Hollman, N. T. Scherrer, A. Cammers-Goodwin and D. Bhattacharyya, *J. Membr. Sci.*, 2004, **239**, 65–79.
25 S. Moya, O. Azzaroni, T. Farhan, V. L. Osborne and W. T. S. Huck, *Angew. Chem., Int. Ed.*, 2005, **44**, 4578–4581.
26 S. Tugulu, A. Arnold, I. Sielaff, K. Johnsson and H.-A. Klok, *Biomacromolecules*, 2005, **6**, 1602–1607.
27 H. Chen and Y. L. Hsieh, *Biotechnol. Bioeng.*, 2005, **90**, 405–413.
28 N. D. Treat, N. Ayres, S. G. Boyes and W. J. Brittain, *Macromolecules*, 2006, **39**, 26–29.
29 T. Wu, P. Gong, I. Szleifer, P. Vlček, V. Šubr and J. Genzer, *Macromolecules*, 2007, **40**, 8756–8764.
30 D. Li, X. Sheng and B. Zhao, *J. Am. Chem. Soc.*, 2005, **127**, 6248–6256.
31 B. Cash, L. Wang and B. C. Benicewicz, *J. Polym. Sci., Part A: Polym. Chem.*, 2012, **50**, 2533–2540.
32 R. Hoogenboom, U. S. Schubert, W. V. Camp and F. E. D. Prez, *Macromolecules*, 2005, **38**, 7653–7659.
33 M. Elladiou and C. S. Patrickios, *Polym. Chem.*, 2012, **3**, 3228–3231.
34 B. Hojjati, R. Sui and P. A. Charpentier, *Polymer*, 2007, **48**, 5850–5858.
35 M. Inoue, S. Fujii, Y. Nakamura, Y. Iwasaki and S. Yusa, *Polym. J.*, 2011, **43**, 778–784.
36 K. Matyjaszewski and J. Xia, *Chem. Rev.*, 2001, **101**, 2921–2990.
37 H. L. Evans, S. N. Lefrak, J. Lyman, R. L. Smith, T. W. Chong, S. T. McElearney, A. R. Schumlan, M. G. Hughes, D. P. Raymond, T. L. Pruett and R. G. Sawyer, *Crit. Care Med.*, 2007, **35**, 89–95.
38 I. Mahapatra, J. Clark, P. J. Dobson, R. Owenc and J. R. Lead, *Environ. Sci.: Processes Impacts*, 2013, **15**, 123–144.
39 H. Dong, J. Huang, R. R. Koepsel, P. Ye, A. J. Russell and K. Matyjaszewski, *Biomacromolecules*, 2011, **12**, 1305–1311.
40 N. Wu, L. Fu, M. Su, M. Aslam, K. C. Wong and V. P. Dravid, *Nano Lett.*, 2004, **4**, 383–386.
41 J. Li, L. Wang and B. C. Benicewicz, *Langmuir*, 2013, **29**, 11547–11553.
42 I. Chaduc, M. Lansalot, F. D'Agosto and B. Charleux, *Macromolecules*, 2012, **45**, 1241–1247.